Numerical Simulations of High-Altitude Aerothermodynamics of a Promising Spacecraft Model

P. Vashchenkov*, M. Ivanov* and A. Krylov†

*Institute of Theoretical and Applied Mechanics SB RAS
†S.P. Korolev Rocket and Space Corporation "Energia"

Abstract. The paper describes a numerical study of aerodynamic characteristics of a re-entry vehicle in the range of altitudes from 120 to 60 km. The computations are performed by the DSMC method with the use of the SMILE software system and by the local bridging method with the use of the RuSat software system. Some computations are performed in an axisymmetric formulation, which makes it possible to estimate the real gas effects (nonequilibrium of internal energy, dissociation of the gas, etc.) on the efficiency of control surfaces. A comparison of results obtained by the local bridging method and the DSMC method allow estimation of the errors of aerodynamic characteristics obtained by the local bridging method.

Keywords: Rarefied Gas Dynamics, DSMC, Bridging Method, Real Gas Effects, Spacecraft Aerodynamics
PACS: 47.27.ek, 47.45.Dt, 47.85.Gj

INTRODUCTION

At the initial stage of space vehicle design, it is necessary to study its aerothermodynamic characteristics in a wide range of free-stream parameters. During de-orbiting, the vehicle passes through the free-molecular flow, then through the transitional zone, and the flight is finalized in the continuum flow. The loads on the vehicle during its descent are considerably changing. The efficiency of control surfaces is also changing. To predict the zone of spacecraft landing, one should know the aerodynamic characteristics of the vehicle at all stages of its descent. The aerothermodynamic characteristics of a promising space vehicle at altitudes from 120 to 60 km are studied in the present work.

PROBLEM PARAMETERS

The aerothermodynamic parameters of the space vehicle at altitudes from 120 to 60 km were studied by the local bridging method. Standard atmosphere parameters were taken for computations. The DSMC method was used to model the flow at several altitudes with the parameters listed in Table 1.

TABLE 1. Parameters of the atmosphere

H, km	**75**	**80**	**85**	**90**	**100**	**110**
M_∞	25.9	26.5	27.2	27.3	26.3	22.5
T_∞, K	208.4	198.6	189.0	186.7	196.6	255.5
ρ_∞, $kg/m^3 \cdot 10^6$	39.9	18.5	8.21	3.42	0.56	0.093

The space vehicle considered is shaped similar to the Apollo capsule. The nose part is spherical, and the rear part is beveled at an angle of 20°. The vehicle geometry is shown in Fig. 1. A qualitative difference from the Apollo capsule is the presence of trimming flaps. One of the objectives of the present activities was to determine the changes in efficiency of these flaps with variations of the angle of attack and with allowance for real gas effects. The temperature of the entire body was assumed to be constant and equal to 1000 K.

The influence of chemical reactions proceeding in the flow on the efficiency of control surfaces was determined in an axisymmetric formulation. As the axisymmetric formulation allows us to obtain the aerodynamic characteristics of only those elements that are obtained by means of rotation by 360°, but the trimming flaps have finite size, their contribution to the aerodynamic parameters was taken into account with the following procedure: the aerodynamic loads (C_X and C_Y) on a circular flap were identified; then the fraction of the loads on the flap in accordance with its

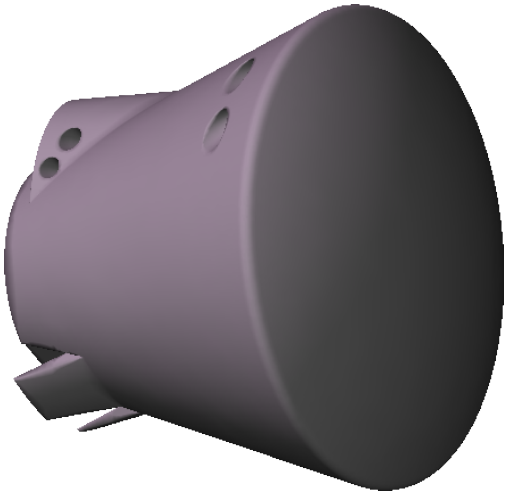

FIGURE 1. Space vehicle geometry

angular size was calculated; finally, the pitching moment generated by the flaps was found from the loads obtained ($C_{X\,flap}$ and $C_{Y\,flap}$).

NUMERICAL METHODS

DSMC

The DSMC computations were performed with the use of the SMILE software system [1]. The internal energy exchange was modeled in accordance with the Larsen–Borgnakke model. Chemical reactions that occur during particle collisions were also taken into account. Diffuse reflection from the surface with complete accommodation of energy was assumed.

The computations were performed on clusters of the Interdepartmental Supercomputer Center (Moscow, Russia) and of the Khristianovich Institute of Theoretical and Applied Mechanics of the Siberian Branch of the Russian Academy of Sciences (Novosibirsk, Russia). Up to 128 processors were used. The computations at an altitude of 75 km required approximately 7000 processor-hours.

Local bridging method

The local bridging method used in this work is based on the technique proposed in [2]. The influence of the flow on an elementary area is described by the following formulas:

$$P = P_0 + P_1 w_n + P_2 w_n^2 \qquad \tau = \tau_0 w_t + \tau_1 w_n w_t \tag{1}$$

Here P and τ are the pressure and friction coefficients of aerodynamic forces normalized to the dynamic pressure $q = \frac{\rho_\infty V_\infty^2}{2}$, $\vec{w}$ is the normalized free-stream velocity vector, and w_n and w_t are the normal and tangential components of the velocity vector to the surface. The parameters P_0, P_1, P_2, τ_0, and τ_1 are calculated using the following formulas:

$$P_0 = P_0^{id} + (P_0^{fm} - P_0^{id})F_{P0} \qquad P_1 = P_1^{fm} F_{P2} \qquad P_2 = P_2^{id} + (P_2^{fm} - P_2^{id})F_{P2} \tag{2}$$

$$\tau_0 = \tau_0^{fm} F_{\tau 0} \qquad \tau_1 = \tau_1^{fm} F_{\tau 1} \tag{3}$$

($\vec{n}$ is the normal vector to the surface and $\vec{\tau}$ is the tangential vector). These vectors lie in one plane.

The bridging coefficients F_{P0}, F_{P1}, F_{P2}, $F_{\tau 1}$, and $F_{\tau 1}$ are used to take into account the influence of the free-molecular or continuum flow regime under particular conditions.

The formulas for calculating the bridging functions F_P and F_τ were derived semi-empirically by Kotov et al. Here we give their final form:

$$F_{P0} = \frac{1}{a\sqrt{\mathrm{Re}_0} + \exp(-b\mathrm{Re}_0)}, \qquad \text{where} \tag{4}$$

$$a = \frac{(\gamma-1)\sqrt{t_w} + \mathrm{M}^{-1}\sqrt{2(\gamma-1)}}{(0.56+1.2t_w)(\mathrm{M}+2.15)} \qquad b = 0.35 + 0.005\mathrm{M} \tag{5}$$

$$F_{P1} = F_{P2} \quad = \quad \exp\left(-(0.125+0.078t_w)\mathrm{Re}_0 \cdot 10^{-1.8(1-\sin\alpha_l)^2}\right) \tag{6}$$

$$F_{\tau 0} = [a_1\mathrm{Re}_0 + \exp(-b_1\mathrm{Re}_0)]^{-3/4}, \qquad \text{where} \tag{7}$$

$$a_1 = \frac{\gamma-1}{2}\left[\sqrt{\frac{\pi\gamma}{2}}\mathrm{M}(0.208+0.341t_w)\right]^{-3/4} \qquad b_1 = 0.213 - 0.133t_w \tag{8}$$

$$F_{\tau 1} = \left[0.145R + \exp\left(7.2\cdot 10^{-3}R - 1.6\cdot 10^{-5}R^2\right)\right]^{-1/2}, \qquad \text{where} \tag{9}$$

$$R = (0.75t_w + 0.25)^{-2/3}\,\mathrm{Re}_0 \cdot 10^{-2.4(1-\sin\alpha_l)^3} \tag{10}$$

RESULTS

DSMC results

Figure 2 shows the pressure fields calculated for non-deflected control flaps and for flaps deflected by 30°. The calculations were performed for a gas without chemical reactions. As it could be expected, the flap influence extends to a fairly small distance upstream, but the field in the wake behind the vehicle is noticeably changed. Thus, for instance, the pressure in the middle of the vehicle base area is approximately 90 Pa for the non-deflected flap and about 50 Pa for the flap deflected by 30°. In a hypersonic flow (M = 25.9), the base pressure does not exert any significant influence on the values of the total aerodynamic coefficients. Flap deflection increases the drag coefficient C_D from 1.50 to 1.54. The lift coefficient is $C_L = 0.103$ for the flap deflected by 30°.

The effect of chemical reactions on the flow field is illustrated in Fig. 3, which shows the pressure fields around the space vehicle obtained in a chemically reacting flow (upper figure) and in a chemically inert gas (lower figure) for the flap deflected by 30°. The calculations were performed for an altitude of 75 km. It is seen that the flow fields are drastically different in the entire computational domain. Indeed, as the major part of the free-stream energy is spent on dissociation of diatomic molecules, the flow temperature in the case of a chemically reacting gas is substantially lower than the temperature obtained with the chemical reactions being ignored. In addition to temperature fields, the Mach number fields are also essentially different. Therefore, we can conclude that the entire flow structure and the shock waves near the vehicle are formed in a different manner.

Figure 4 shows the distributions of temperature and pressure normalized to the free-stream pressure over the stagnation lines at altitudes of 75, 85, and 90 km. The plots show the stagnation lines obtained for chemically reacting and chemically inert gases. The plots on the left show the free-stream parameters, and the plots on the right show the situation with the body located at $X = 0$. It is seen that the temperature of the flow behind the bow shock wave is substantially lower if chemical reactions are taken into account. In addition, the stand-off distance of the bow shock wave is changed. The influence of chemical reactions becomes attenuated with increasing flight altitude. Thus, for instance, the difference in the shock-wave stand-off distance is 0.187 m at an altitude of 75 km, 0.133 m at 85 km, and 0.093 m at 90 km.

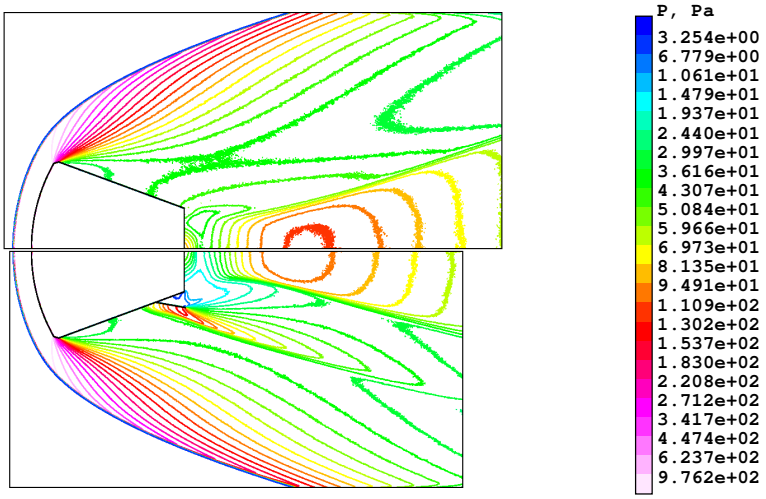

FIGURE 2. Pressure fields. Altitude 75 km. Chemically inert gas. Non-deflected flap (upper) and flap deflected by 30°(downer).

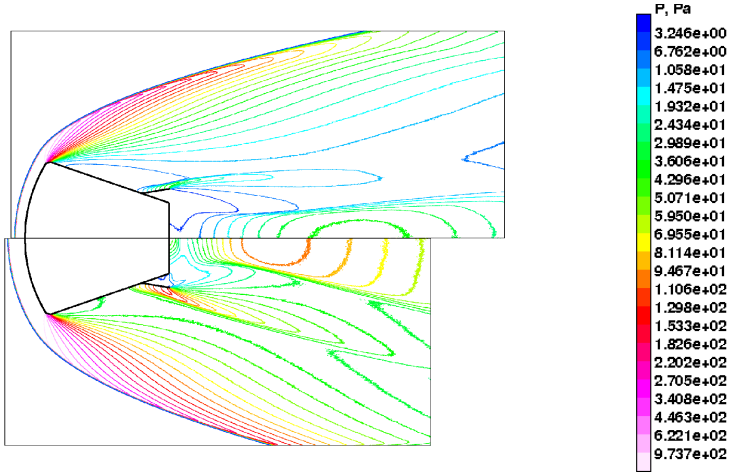

FIGURE 3. Pressure fields. Altitude 75 km. Flap deflection angle 30°. Chemically reacting gas (upper figure) and chemically inert gas (lower figure).

At altitudes from 75 to 90 km, the space vehicle moves in the flow regime close to continuum (the Knudsen number changes from $3.7 \cdot 0^{-4}$ to $4.3 \cdot 10^{-3}$). The drag coefficient C_D at altitudes from 75 to 90 km is almost independent of the flight altitude and the presence of chemical reactions; its value is approximately 1.55. The heat-transfer coefficients $C_h = \frac{Q}{\frac{\rho_\infty V^3}{2} S^*}$ obtained in computations with and without chemical reactions are listed in Table 2. It is seen from the Table that the heat-transfer coefficient decreases by more than a factor of 3 at an altitude of 75 km and by a factor of 2 at an altitude of 90 km if chemical reactions are taken into account.

To determine the efficiency of control surfaces, we performed three-dimensional computations of spacecraft aerodynamics with the flap deflected by 0, 20°, and 30°at altitudes from 80 to 110 km for angles of attack 0 and 40°. As

TABLE 2. Heat-transfer coefficient C_h of the vehicle. DSMC results. Non-deflected flaps. Axisymmetric model

Altitude, km	**75**	**80**	**85**	**90**
Chemically reacting flow	$1.30 \cdot 10^{-2}$	$2.11 \cdot 10^{-2}$	$3.38 \cdot 10^{-2}$	$6.18 \cdot 10^{-2}$
Chemically inert flow	$4.30 \cdot 10^{-2}$	$6.22 \cdot 10^{-2}$	$9.47 \cdot 10^{-2}$	$1.36 \cdot 10^{-1}$

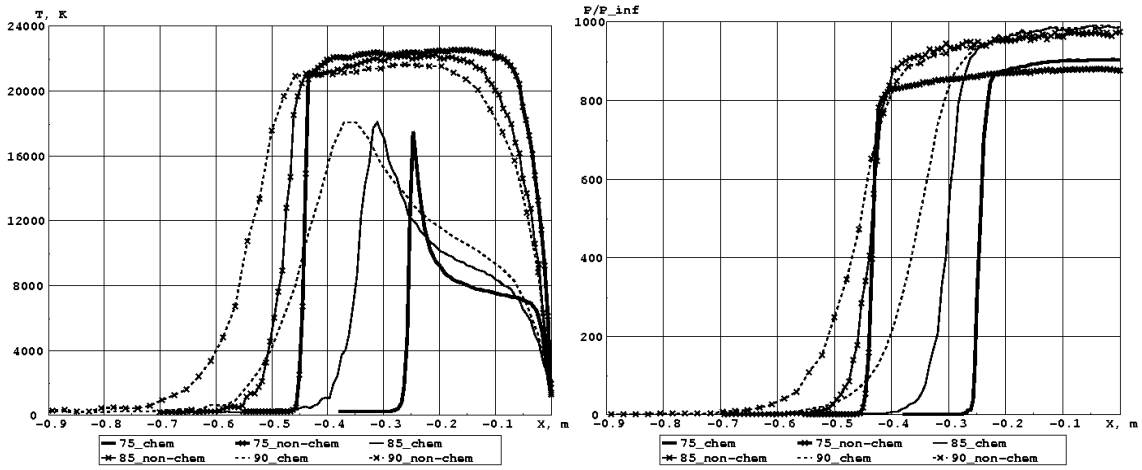

FIGURE 4. Temperature (left) and pressure (right) along the stagnation line at different altitudes. Axisymmetric computation.

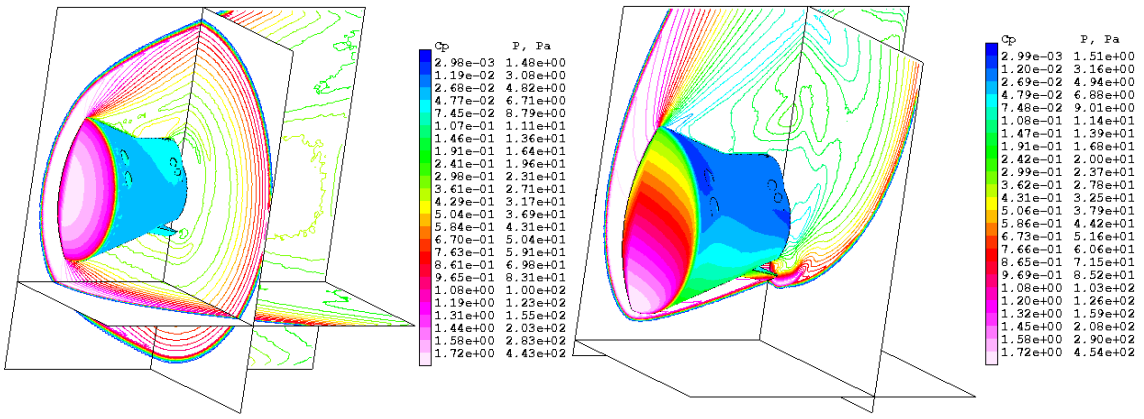

FIGURE 5. Pressure field and surface distribution of the pressure coefficient. Altitude 80 km. Flap deflection angle 30°. Angle of attack: 0 (left) and 40°(right)

an example, Fig. 5 shows the pressure field and the surface distribution of the pressure coefficient at an altitude of 80 km at a zero angle of attack and 40°. It is seen from these figures that the control flap induces an extremely weak perturbation into the flow at a zero angle of attack, but its influence on the flow field becomes fairly significant as the angle of attack is increased to 40°.

Results of the local bridging method

The DSMC method is too expensive to perform a multiparametric study of aerothermodynamic characteristics of the space vehicle at different angles of attack, different altitudes, and different angles of flap deflection.

For this reason, another series of computations was performed by the engineering local bridging method. To estimate their accuracy, the results of these computations were compared with the DSMC results. Figure 6 shows the aerodynamic characteristics as functions of the angle of attack for a flap deflection angle of 30°. The curves show the results for the angle of attack equal to 0 (1), 10 (2), 20 (3), 30 (4), and 40°(5). Dahsed curves 6 and 7 show the results of the 3D DSMC computations for the angles of attack equal to 40°and 0, respectively. There is no curve that refers to the zero angle of attack in the $C_N(H)$ plot, because the normal force is close to zero at the zero angle of attack. The moment characteristic differs from zero, because the center of gravity is shifted down on 0.156 m from the spacecraft axis. The curves obtained by the engineering method describe the aerodynamic coefficients in the range of altitudes

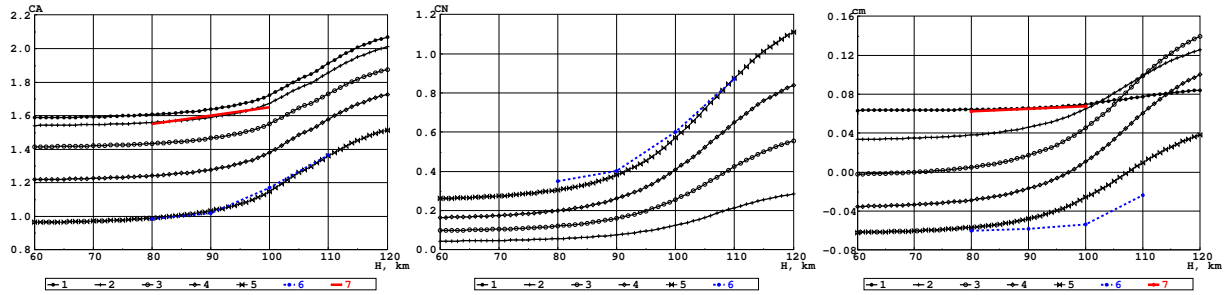

FIGURE 6. Axial and normal force coefficients and pitching moment coefficient versus altitude for different angles of attack. Flap deflection angle 30°. Angle of attack 0°(1), 10°(2), 20°(3), 30°(4), and 40°(5); DSMC results for the angle of attack equal to 40°(6) and 0°(7).

between 120 and 60 km. The difference from the DSMC results is approximately 5% for the force characteristics. The accuracy of the moment characteristics is lower, especially at an angle of attack of 40°at altitudes of 100 and 110 km (about 50%). It should be mentioned, however, that the value of the pitching moment coefficient is close to zero, and the large relative difference actually means insignificant absolute difference in the pitching moment coefficient.

CONCLUSIONS

The paper describes the results of numerical simulations of high-altitude aerothermodynamics of a re-entry space vehicle. The DSMC computations reveal a significant effect of chemical reactions on the flow fields around the spacecraft and on the heat-transfer coefficient at altitudes below 90 km. Because of considerable changes in the flow structure near the base surface of the spacecraft, there is a several-fold difference in the values of the pitching moment and the lift force of the vehicle with deflected control surfaces, which were obtained with and without chemical reactions. Simultaneously, chemical reactions proceeding in the gas exert practically no effect on the drag coefficient. The changes in the aerodynamic characteristics with variations of the angle of attack and the angle of flap deflection at altitudes from 80 to 110 km were computed by the DSMC method. The aerodynamic characteristics of the spacecraft at altitudes from 120 to 60 km were also calculated by the engineering local bridging method. Comparisons with the DSMC results showed that the axial and normal force coefficients are calculated rather accurately (within 5%). The results obtained can be used to design the thermal protection system of the space vehicle and to construct its de-orbiting trajectory.

ACKNOWLEDGMENT

This work was supported by the Lavrentyev Youth Grant ”High-altitude aerothermodynamics of advanced spacecraft taking into account non-equilibrium chemical reactions“ and by the Russian Foundation for Basic Research (Grant No. 09-07-00480-a).

REFERENCES

1. M.S. Ivanov, G.N. Markelov, and S.F. Gimelshein. Statistical simulation of reactive rarefied flows: numerical approach and aplplications. In *Proc. 7th Joint Thermophysics and Heat Transfer Conf.*, 1998. AIAA Paper 98–2669.
2. V.M. Kotov, E.N. Lychkin, A.G. Reshetin, and A.N. Shelkonogov. An approximate method of aerodynamics calculation of complex shape bodies in a transition region. In *Proc. 13th Int. Conf. on Rarefied Gas Dynamics*, volume 1, pages 487–494. Plenum Press, 1982.